Hindawi Publishing Corporation
Advances in Mechanical Engineering
Volume 2013, Article ID 902874, 8 pages
http://dx.doi.org/10.1155/2013/902874

Research Article

Fluid Dynamics in a Teniente Type Copper Converter Model with One and Two Tuyeres

Alvaro Valencia,[1] Marco Rosales-Vera,[2] and Camilo Orellana[1]

[1] *Department of Mechanical Engineering, Universidad de Chile, Beaucheff 850, Santiago 8370448, Chile*
[2] *Institute for Innnovation in Mining and Metallurgy, Ahumada 341, Santiago 8320181, Chile*

Correspondence should be addressed to Alvaro Valencia; alvalenc@ing.uchile.cl

Received 8 March 2013; Revised 6 June 2013; Accepted 6 June 2013

Academic Editor: Oronzio Manca

We have numerically studied the fluid dynamics in a model of Teniente type copper converter with combined lateral and bottom gas injection. The three-dimensional simulation of the two-phase system was carried out using the volume of fluid (VOF) and the standard k-ε turbulence models implemented in the commercial solver Fluent. The numerical investigation was carried out in a 1 : 5 scaled water slice model for three different gas injection Froude numbers of the bottom tuyere (0, 36, and 64). The submerged gas injection produces a turbulent jet and provides efficient mixing of the gas and liquid phases. The gas injection through a bottom tuyere increases the fluid mixing, and for Froude number of Fr = 64 interactions between the two gas jets were found.

1. Introduction

The Teniente copper converter was conceived in the early 70s in Codelco Chile, and the first unit was commissioned in 1977 in Caletones foundry. Important improvements and operational changes have showed that this reactor is an alternative for the smelting and converting operations [1]. Actually, this reactor can smelt up to 2,400 tons per day of concentrate, and the goal is to explore the possibility to process up to 3,000 tons per day of concentrate. The gas injected through the submerged tuyere line in Teniente converter produces into the bath of molten matte a three-phase highly turbulent flow. The air flow rate determines the processes occurring in the converter such as converting rate, oxygen efficiency, mixing, splashing, and accretion build-up. Despite the importance of the interaction of the air jet and the matte in the conversion process, few studies of the fluid dynamics of converting process have been reported in the literature.

Themelis et al. [2] derived an equation to describe the trajectory of a gas jet in a liquid. They reported theoretical and experimental results for air jets injected into water and matte for different Froude numbers. Hoefele and Brimacombe [3] have experimentally studied the behavior of gas discharging into a liquid in laboratory and in plant. Two flow regimes, bubbling and steady jetting, have been distinguished as a function of the Froude number based on tuyere diameter, Fr, and the ratio of gas to liquid densities. They have correlated the forward penetration of the jets, l, with the equation: $l/d = 10.7\mathrm{Fr}^{0.92}(\rho_g/\rho_l)^{0.35}$. They concluded that low pressure blowing has the disadvantage of poor air penetration into the bath so that the jets rise close to the back wall and locally accelerate refractory wear. Zhao and Irons [4] reported the transition from bubbling regime to jetting regime when gas is injected into liquid at high velocity through submerged tuyeres. They found that the critical injection velocity for instability depends on surface tension, tuyere diameter, and the gas-to-liquid density ratio, which can be summarized by $\mathrm{We} = 10.5(\rho_g/\rho_l)^{-0.5}$, where We is the Weber number.

The gas fraction and bubble frequency distributions in a submerged air jet, injected horizontally into mercury, have Oryall and Brimacombe [5] measured under isothermal conditions, and the results reveal that the jets expand extremely rapidly upon discharge from the tuyere. They concluded that air jets injected into copper converters expand rapidly and penetrate only a short distance into the bath. Thus, rather than reacting in the middle of the bath, the jets may be impinging on the back wall refractory and contributing to the erosion observed there. The injection phenomena in

a Peirce-Smith copper converter and a slag furnace have been investigated by Bustos et al. [6]. They have found that in both processes if the tuyeres are shallowly submerged the gas may channel directly to the bath surface with low retention time in the liquid phase. Liow and Gray [7] studied experimentally in a 1:10 scaled water model of a Peirce-Smith copper converter the influence of bath depth and tuyere submergence on the formation of standing waves on bath surface. They concluded that the wave steepness is responsible for the changes in standing waves mode and can contribute to the splashing of liquid from the first asymmetric standing wave if the amplitude of the wave is large.

Rosales et al. [8] have conducted numerical simulations to study the gravity waves produced on bath free surface in the Teniente converter. The results show a good correlation with the experimental data. Longitudinal waves were formed due to the reflection and transmission of waves generated in the tuyere line zone. A theory for slopping control in the Teniente converter was proposed by Rosales et al. in [9]. The control includes gas injection with two submerged tuyere lines. The second tuyere line should be located in converter bottom. Theoretically, the ascending air column in the central bath zone interferes with the asymmetric surface wave, providing more bath stability.

The experimental investigation of a methodology for controlling slopping in copper converters by using lateral and bottom gas injection was discussed in [10]. They conclude that air injection with two tuyere lines reduces slopping. An injection system with two tuyere lines allows wave diminishment within the reactor, which stabilizes the metallurgical process, decreases refractory damage, and permits a more extensive period of operation.

The CFD simulation in a copper converter with bottom injection was reported by Gonzalez et al. [11]; they found up a bubbling regime, and they suggest that relationship between air inlet velocity and bath mixing is not linear. This means that very high air velocities are not necessary to obtain adequate copper matte mixing conditions. The CFD modelling of mixing in a Peirce-Smith converter has been reported by Chibwe et al. [12]; there exists a critical slag thickness in the converter model, above which, increasing air flow rate results in extended mixing times in the simulated slag. The spashing in a copper model was investigated by Koohi et al. [13], the effects such as blowing angle, volumetric flow rate of air and the distance of the blowers from water were studied.

In a previous work, Valencia et al. [14] studied the fluid dynamics in a slice water model of the Teniente type copper converter with one submerged tuyere. We study the influence of Froude number on bath dynamics in particular with regard to flow mixing in the bath, jet stability and splashing. The flow is characterized with an unsteady jet, which moves into back wall direction and in some instants collapses. Recently, we have studied the fluid dynamics in a Teniente type copper converter including white metal and slag liquid phases and gas phase through air injection from 50 submerged tuyeres [15]. Experimental observation of the phenomena was carried out in a 1:5 scaled water vessel, and mean frequencies and amplitudes of bath surface oscillation were determined in four characteristic points of bath surface.

In the present work, we study numerically the fluid dynamics in a slice model of Teniente type copper converter with combined lateral and bottom air blowing using submerged tuyeres. The numerical investigation was carried out in a 1:5 scaled water slice model for three different gas injection Froude numbers of the bottom tuyere (0, 36, and 64). The hypothesis to probe is that an increase in the fluid mixing without important increase of surface kinetic energy, due the simultaneous operation of a lateral and bottom tuyere, can be reached, and in this way the conversion potential of the reactor can be considerably increased.

2. Mathematical Model and Geometry

In the volume of fluid (VOF) formulation, [16], for multiphase fluid dynamics the fluids are not interpenetrating. For each phase, a variable is introduced: the volume fraction of the phase in the computational cell. In each control volume, the volume fractions of all phases sum to unity. The fields for all variables and properties are shared by the phases and represent volume-averaged values, as long as the volume fraction of each of the phases is known at each location. Thus, the variables and properties in any given cell are either purely representative of one of the phases or representative of a mixture of the phases, depending upon the volume fraction values.

The VOF model uses the mass and momentum conservation equations for incompressible fluids, to describe the fluid dynamics of both gas and liquid phase, that is,

$$\vec{\nabla} \cdot \vec{u} = 0,$$
$$\frac{\partial \rho \vec{u}}{\partial t} + \vec{\nabla} \cdot \rho \vec{u} \cdot \vec{u} = -\vec{\nabla} p + \mu_{\text{eff}} \nabla^2 \vec{u} + \rho \vec{g}. \tag{1}$$

Here the properties of a fluid are given by

$$\rho(\vec{x}, t) = F(\vec{x}, t)\, \rho_l + [1 - F(\vec{x}, t)] \cdot \rho_g,$$
$$\mu_{\text{eff}}(\vec{x}, t) = F(\vec{x}, t)\, \mu_{l,\text{eff}} + [1 - F(\vec{x}, t)] \cdot \mu_{g,\text{eff}}. \tag{2}$$

F is the local volume fraction of one fluid. Its value is one in the liquid phase and zero in the gas phase. A value between 1 and 0 indicates a density interface. The subscripts l and g indicate liquid and gas phases, respectively. The force due to surface tension acting on the gas-liquid interface was considered negligible in the present formulation. The model solves the scalar advection equation for the quantity F; this equation states that F moves with the fluid:

$$\frac{\partial F}{\partial t} + \vec{u} \cdot \vec{\nabla} F = 0. \tag{3}$$

In this work, the standard k-ε turbulence model, extended for the use in multiphase systems, has been used [17]. This is a two equation model based on transport equations for the turbulence kinetic energy, k, and its dissipation rate ε.

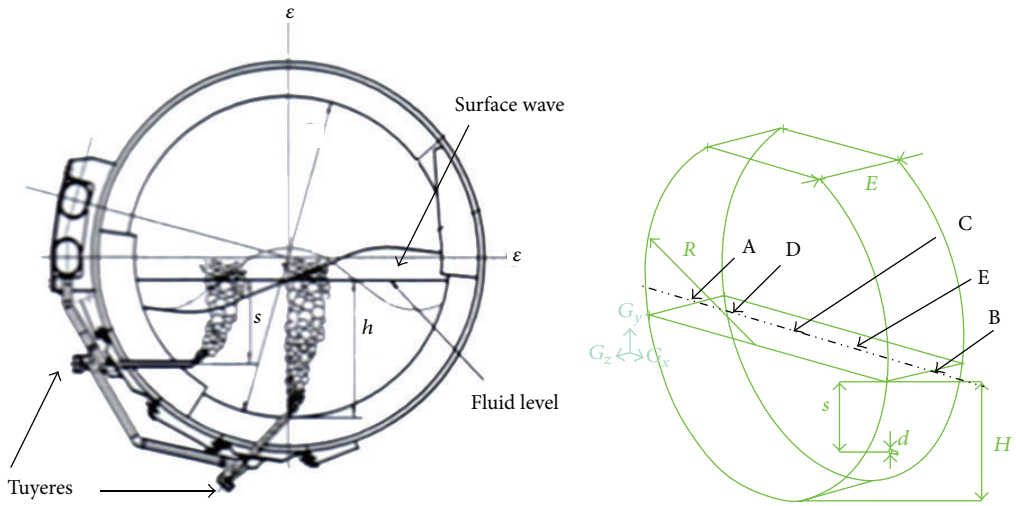

Figure 1: Geometry of Teniente type copper converter slice model: (a) conceptual model with two tuyeres; (b) principal dimensions.

The equations for turbulent kinetic energy k and its dissipation rate ε are

$$\frac{\partial}{\partial t}(\rho k) + \frac{\partial}{\partial x_i}(\rho k u_i) = \frac{\partial}{\partial x_j}\left[\left(\mu + \frac{\mu_t}{\sigma_k}\right)\frac{\partial k}{\partial x_j}\right] + G_k - \rho\varepsilon,$$

$$\frac{\partial}{\partial t}(\rho\varepsilon) + \frac{\partial}{\partial x_i}(\rho\varepsilon u_i) = \frac{\partial}{\partial x_j}\left[\left(\mu + \frac{\mu_t}{\sigma_\varepsilon}\right)\frac{\partial \varepsilon}{\partial x_j}\right] + C_{1\varepsilon}\frac{\varepsilon}{k}G_k - C_{2\varepsilon}\rho\frac{\varepsilon^2}{k}. \quad (4)$$

In these equations, G_k represents the generation of turbulence kinetic energy due to the mean velocity gradients, $C_{1\varepsilon}$, $C_{2\varepsilon}$, σ_k, and σ_ε are model constants. These values have been determined from experiments with air and water for fundamental turbulent shear flows including homogeneous shear flows and decaying isotropic grid turbulence. In this model, the effective viscosity in the momentum equations is the sum of the molecular and turbulent viscosity:

$$\mu_{\text{eff}} = \mu + \mu_t \quad (5)$$

with

$$\mu_t = \rho C_\mu \frac{k^2}{\varepsilon}. \quad (6)$$

We have set for air a density $\rho_g = 1.225$ [kg/m^3] and a viscosity $\mu_g = 1.79 \times 10^{-5}$ [kg/ms]; for the water we have used a density $\rho_l = 998$ [kg/m^3] and a viscosity $\mu_l = 1 \times 10^{-3}$ [kg/ms]. The surface tension was set to $\sigma = 0.072$ [N/m].

Figure 1 shows the geometry of Teniente type copper converter slice model with the principal dimensions scaled 1 : 5. It is a cylindrical vessel of $E = 0.227$ m thickness with an inner radius of $R = 0.421$ m, and it is filled with water with $H = 0.35$ m to simulate the actual converter operation condition. The submergence of the lateral tuyere is $s = 0.2$ m, and the tuyere diameter is $d = 0.0078$ m. The Froude number for the lateral tuyere is Fr = 100. Three different Froude numbers for the bottom tuyere were considered Fr = 0, 36, and 64; see Table 1. For the tuyeres, the turbulence intensity can be estimated from the following formula derived from an empirical correlation for turbulent pipe flows [17]:

$$I = \frac{u'}{u_0} = 0.16\,\text{Re}^{-1/8}. \quad (7)$$

With a tuyere Reynolds number of Re = 42,138, the turbulence intensity is 4%, according to (7). For complex flows with multiple inlets, it is recommended to specify the inlet value of k-ε in terms of the turbulence intensity to represent fully-developed turbulence; k can be computed with (8), [17]:

$$k = 1.5(Iu_0)^2. \quad (8)$$

Finally, standard wall functions are employed to prescribe the boundary conditions along the walls in the computational domain. The standard wall functions are widely used for industrial flows [17]. In the range of y^+, defined in (9), between $30 < y^+ < 300$ turbulence plays a major role, and the near wall model approach is correct; the grid size was chosen so that in the large part of the converter walls the value of y^+ is set in this range. Figure 2 shows the contours of wall y^+ for

Table 1: Injection conditions for the lateral and bottom tuyeres.

Model	Fr lateral tuyere	Fr bottom tuyere	v lateral tuyere (m/s)	v bottom tuyere (m/s)
I	100	0	78.9	0
II	100	36	78.9	47.3
III	100	64	78.9	63.1

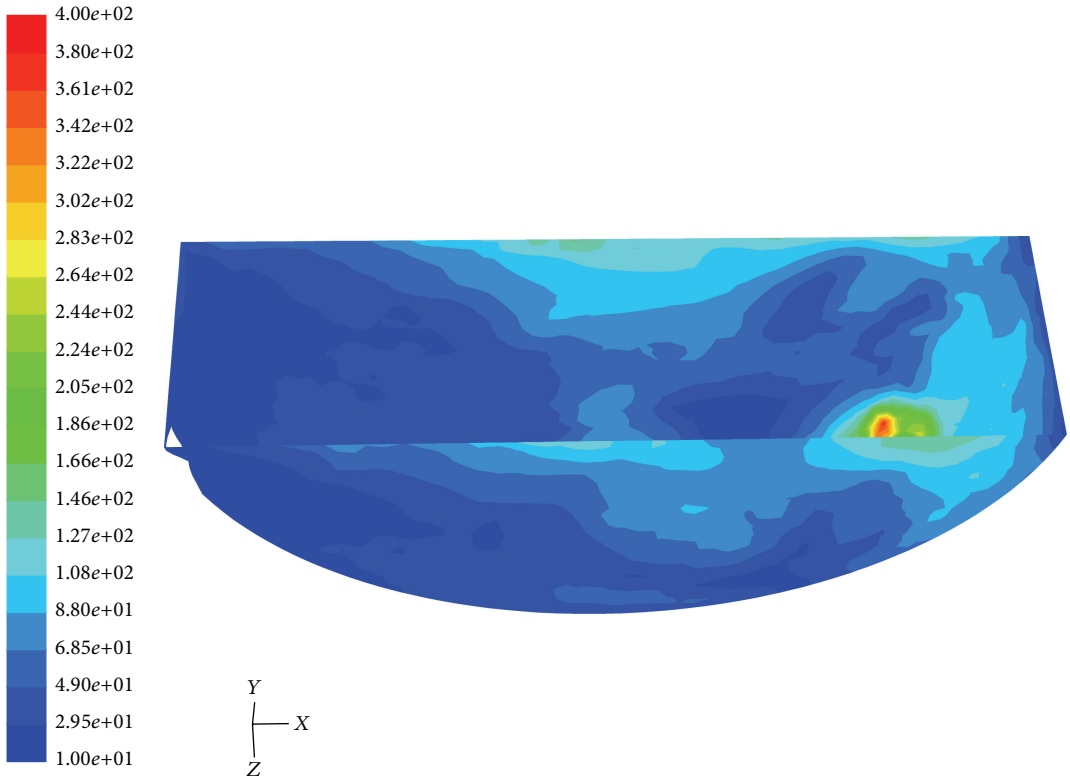

Figure 2: Contours of wall y^+ for the model III.

the model III; only in the tuyere zone the y^+ values are larger as recommended:

$$y^+ = \frac{\rho y_P}{\mu}\sqrt{\frac{\tau_w}{\rho}}. \quad (9)$$

3. Numerical Setup

The VOF and the k-ε turbulence models were solved using the commercial solver Fluent 6.3.26 on 64-bit. This package is a finite volume solver using body-fitted computational grids. Fluent uses a colocated scheme, whereby pressure and velocity are both stored at cell centers [17]. The pressure velocity coupling is obtained using the SIMPLEC algorithm. We use the geometrical reconstruction scheme to obtain the faces fluxes, when the cell is near the interface between two phases; this scheme represents the interface between fluids using a piecewise-linear approach [16].

For the time-dependent VOF calculations, we use a second order implicit time-marching scheme with a convergence criteria of 0.001 and with a time step $\Delta t = 1 \times 10^{-4}$ s. The algorithm used for pressure discretization was PRESTO, and for the momentum, turbulent kinetic energy and its dissipation rate equations second order upwind scheme were used [17].

The time step was chosen, so that in each time step the convergence criterion of the residuals of continuity and Navier-Stokes 0.001 was reached; we have set a maximum of 20 iterations in each time step; for large time step, the convergence was not reached, and the solutions were dropped.

Table 2: Mass weighted averaged velocity, cell Reynolds number and dynamic pressure in the model I for five different cells number for the time of 5 s.

Cells number	Average velocity (m/s)	Cell Reynolds number	Average dynamic pressure (N/m^2)
48463	0.210	6.61	36.70
71159	0.130	4.94	15.21
112917	0.151	5.62	18.27
150743	0.134	5.64	14.87
205805	0.126	5.04	13.70

To verify grid independence, numerical simulations based on the model I with one active tuyere were performed on five different grid sizes. Table 2 shows mass weighted averaged velocity, cell Reynolds number, and dynamic pressure in the model including air and water for the time of 5 s. Between the two finer grid sizes, the difference of predictions of average velocity, cell Reynolds number, and dynamic pressure is 6.3%, 12%, and 8.5%, respectively. Considering that computational time increases linearly with grid size, we used the grid with 150,743 control volumes for the simulations.

The workstation used to perform the simulations in this work is based on an Intel Pentium IV processor of 3.4 GHz clock speed, 3.0 GB RAM memory, 64 bits, and running on

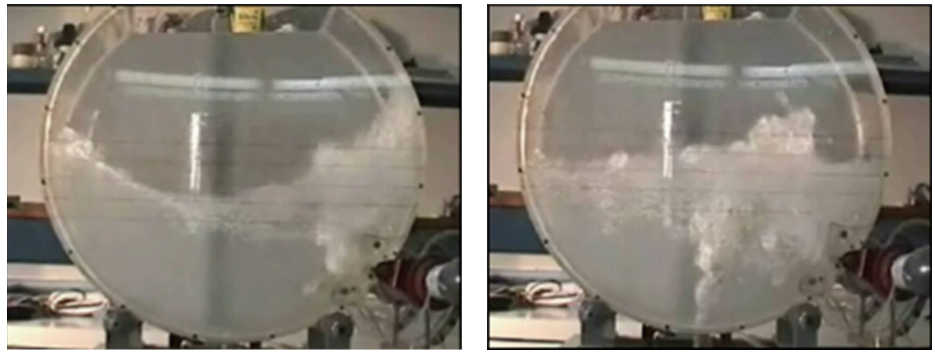

(a) (b)

Figure 3: Photographs in water models of bath oscillation: (a) slice model with one tuyere and (b) slice model with two tuyeres, [10].

the Linux SUSE 10.0 operating system. The simulation time for one model based on 10 s employing 10^{-4} time steps was approximately 10 days of CPU.

4. Results and Discussion

Experimental visualizations of the fluid dynamics in a slice model of the Teniente copper converter scaled 1 : 5 were obtained in [10]. Pictures were recorded with a digital video camera for later analysis. The water level was set to $H/R = 0.83$, and the Froude number based on tuyere diameter was set to 100. Figures 3(a) and 3(b) show the normal operation of the reactor in the slice with one and two tuyeres, respectively.

Figure 4 shows the volume fraction of water distribution and the velocity vectors colored by magnitude in the half plane of the slice models I, II, and III for the time of 8.5 s. The submerged gas injection with a lateral tuyere produces a bubbling regime, moderate agitation of bath surface, and limited gas penetration into the bath; the jet formed shows the characteristics of low water penetration and jet instability; the corresponding velocity vectors show a strong vortex only on the back wall and low recirculation in the bath middle, Figures 4(a) and 4(b).

The air injection through the bottom submerged tuyere produces important changes in the fluid dynamics characteristics of the bath. With Fr = 36, the jets are independent, and the produced bath mixing reaches more than the half space of bath; see Figure 4(d). The formed vortices have higher intensity, and the bath surface is more perturbed; see Figures 4(c) and 4(d). With Fr = 64, the second air jet produces more defined bath surface wave, jet interaction, bath inner agitation, and mixing; see Figures 4(e) and 4(f). The results show, that the Teniente type copper converter can operate with two submerged tuyeres and with this Froude numbers in an efficient way.

To calculate the principal frequency of bath standing wave, the vertical velocity in point A (see Figure 1(b)) was recorded in model I. Figure 5 shows the power density spectrum obtained with the fast Fourier transform for this velocity in point A. The principal frequency is $f = 1.3$ Hz. A theoretical dimensionless frequency α was obtained in [8] for the principal standing waves modes in cylindrical vessels.

$$\alpha^2 = (2\pi f)^2 \frac{D}{2g} = \frac{n\pi}{4((H/D)(1-H/D))^{0.5}} \tanh\left(\frac{n\pi}{2}\left(\frac{H/D}{1-H/D}\right)^{0.5}\right). \quad (10)$$

Using (10) for the model I, we obtain $f_1 = 0.9$ Hz and $f_2 = 1.36$ Hz. The numerical frequency matches the theoretical frequency f_2.

To quantify the effect of the submerged air injection through the bottom tuyere on bath surface, the specific kinetic energy in five representative points on bath surface (see Figure 1(b)) was calculated for 10 s of operation time. Figure 6 shows the specific kinetic energy for the three models. In points A, B, and D, the kinetic energy is very low; in point C, the kinetic energy for the model II and III is similar; the large values for model II and III are due to that point C is in the position of vertical injection. In point E, the specific kinetic energy is nearly the same for the three models. It is concluded that the vertical gas injection through a second tuyere does not produce important increases of bath surface kinetic energy, and therefore the risk of bath slopping is not increased.

The present investigation uses a water-air model with the assumption of incompressible fluid; in a real molten copper-air case in a full-scaled model, we should use different properties for white metal and slag phases and for the gas we should use the gas ideal equation, to include the liquid-gas interactions.

To apply the bottom injection in copper converter, more investigations are needed to study the gas injection in a bath of matte and slag in a scaled converter; also a new punching machine capable of cleaning the bottom tuyere line must be developed.

5. Conclusions

The gas injection in a Teniente copper converter is critical for the metallurgical process; a new gas injection method

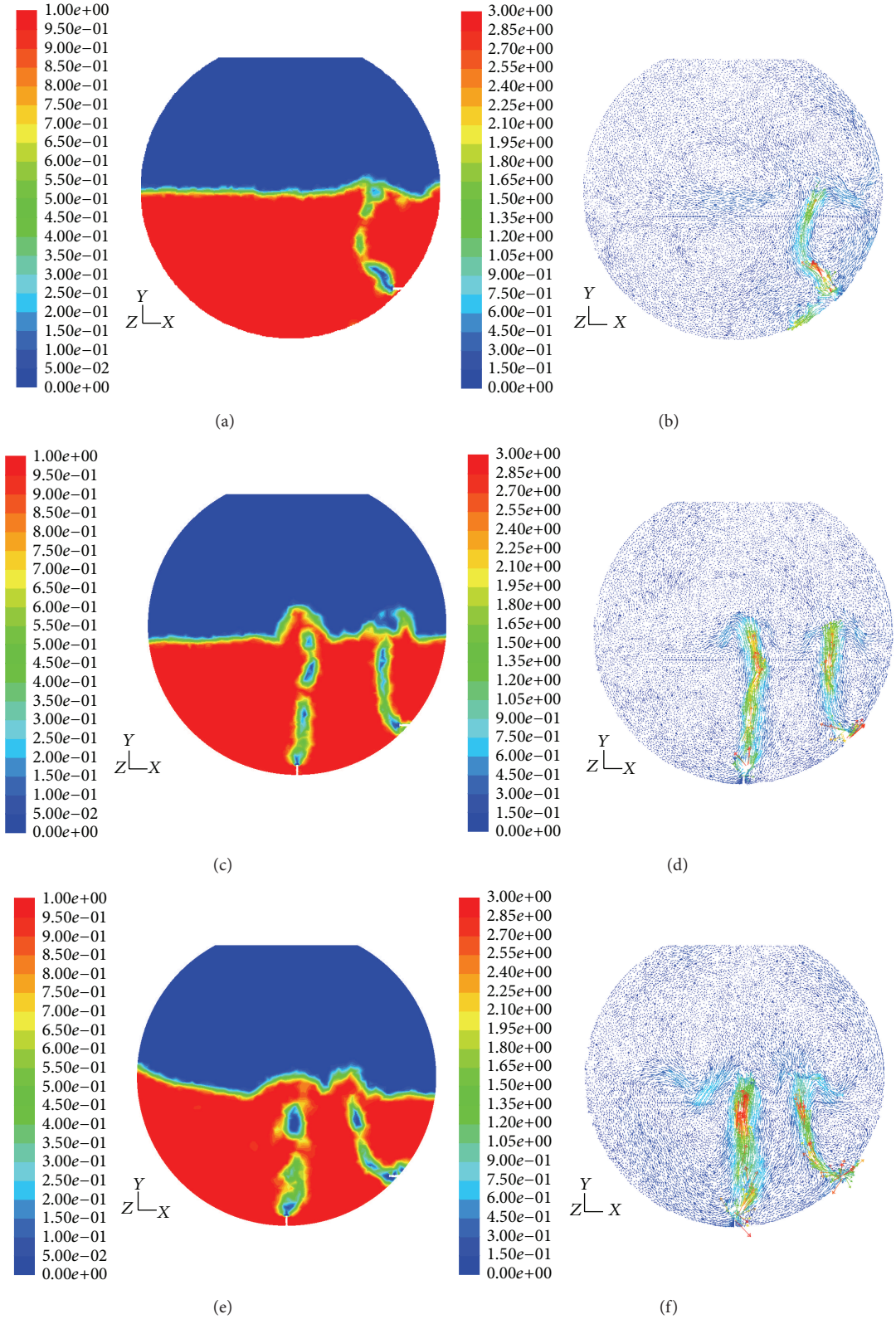

Figure 4: Distributions of volume fraction of water at middle plane for the time of 8.5 s: (a) model I, (c) model II, and (e) model III for the time of 8.5 s. Velocity vectors at middle plane for the time of 8.5 s: (b) model I, (d) model II, and (f) model III.

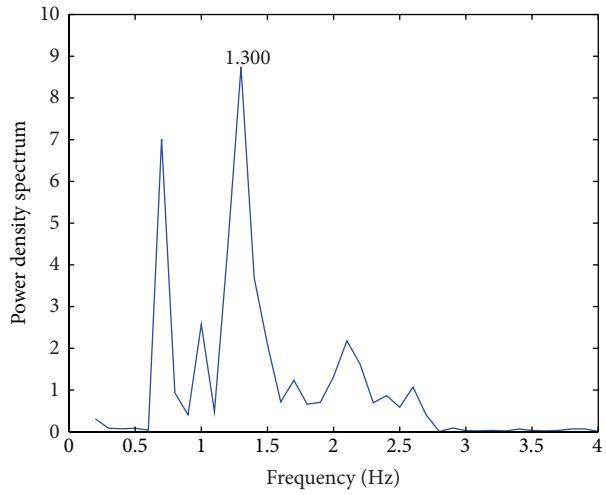

Figure 5: Power density spectrum of vertical velocity in point A of middle plane in model I.

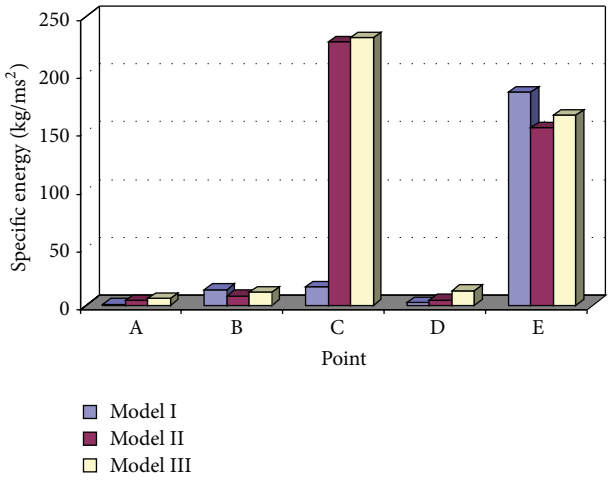

Figure 6: Time averaged specific kinetic energy over 10 s of operation time for five selected points in models I, II, and III.

through two submerged tuyeres was investigated in this work, for different Froude numbers. We have found an increase in the fluid mixing without important increase of surface kinetic energy due the simultaneous operation of the lateral and bottom tuyeres. From the fluid dynamical point of view, a relevant increase in the air flow rate can be reached in copper converters through the operation of two submerged tuyeres lines without an increase of bath instability.

Nomenclature

d: Tuyere diameter, m
E: Slice model thickness, m
f: Frequency, Hz
F: Volume fraction of one fluid
Fr: Tuyere modified Froude number, $u_o^2/[g(\rho_l/\rho_g - 1)d]$
g: Gravity acceleration, m s^{-2}
H: Water depth, m
k: Turbulent kinetic energy, m^2 s^{-2}
l: Jet penetration, m
p: Pressure, Pa
R: Model radius, m
Re: Tuyere Reynolds number, $\rho_g u_o d/\mu_g$
s: Tuyere submergence, m
t: Time, s
u: Velocity, m s^{-1}
u_o: Mean velocity of gas in tuyere, m s^{-1}
We: Tuyere Weber number, $\rho_g u_o^2 d/\sigma$
x: Position, m
y^+: Nondimensional distance to wall.

Greek Symbols

ε: Turbulent dissipation rate, m^2 s^{-3}
μ_t: Turbulent viscosity, kg m^{-1} s^{-1}
μ: Viscosity kg m^{-1} s^{-1}
μ_{eff}: Effective viscosity mixture, kg m^{-1} s^{-1}
$\mu_{l,\text{eff}}$: Effective viscosity liquid phase, kg m^{-1} s^{-1}
$\mu_{g,\text{eff}}$: Effective viscosity gas phase, kg m^{-1} s^{-1}
ρ: Density mixture, kg m^{-3}
ρ_l: Density liquid phase, kg m^{-3}
ρ_g: Density gas phase, kg m^{-3}
σ: Surface tension coefficient, N m^{-1}
τ_w: Wall shear stress, Pa.

Acknowledgment

This work was partially supported by Grant PFB03 2007 CMM, Universidad de Chile, CONICYT, Chile.

References

[1] P. C. Morales and R. S. Mac-Kay, "Upgrading of the Teniente technology," in *Proceedings of the 4th International Conference COPPER (COBRE '99)*, pp. 161–171, Phenix, Ariz, USA, October 1999.

[2] T. N. Themelis, T. P. Tarassoff, and S. J. Szekely, "Gas-liquid momentum transfer in a copper converter," *Transactions of the Metallurgical Society of AIME* , vol. 245, no. 11, pp. 2425–2433, 1969.

[3] E. O. Hoefele and J. K. Brimacombe, "Flow regimes in submerged gas injection," *Metallurgical Transactions B*, vol. 10, no. 4, pp. 631–648, 1979.

[4] Y.-F. Zhao and G. A. Irons, "The breakup of bubbles into jets during submerged gas injection," *Metallurgical Transactions B*, vol. 21, no. 6, pp. 997–1003, 1990.

[5] G. N. Oryall and J. K. Brimacombe, "The physical behavior of a gas jet injected horizontally into liquid metal," *Metallurgical Transactions B*, vol. 7, no. 3, pp. 391–403, 1976.

[6] A. A. Bustos, G. G. Richards, N. B. Gray, and J. K. Brimacombe, "Injection phenomena in nonferrous processes," *Metallurgical Transactions B*, vol. 15, no. 1, pp. 77–89, 1984.

[7] J.-L. Liow and N. B. Gray, "Slopping resulting from gas injection in a peirce-smith converter: water modeling," *Metallurgical Transactions B*, vol. 21, no. 6, pp. 987–996, 1990.

[8] M. Rosales, P. Ruz, R. Fuentes, A. Valencia, A. Moyano, and J. Bobadilla, "Gravity waves in the Teniente converter," in *Pyrometallurgy of Copper*, vol. 4, book 2, pp. 485–498, Santiago, Chile, 2003.

[9] M. Rosales, C. Leon, R. Fuentes, A. Valencia, A. Moyano, and C. Caballero, "A theory of slopping by gas injection in Teniente converter," in *Proceedings of the The Carlos Diaz Symposium on Pyrometallurgy*, vol. 3, book 1, pp. 413–424, Toronto, Canada, 2007.

[10] M. Rosales, A. Valencia, and R. Fuentes, "A Methodology for controlling slopping in copper converters by using lateral and bottom gas injection," *International Journal of Chemical Reactor Engineering*, vol. 7, no. 1, article A21, 2009.

[11] J. Gonzalez, C. Real, M. Palomar-Pardave, L. Hoyos, M. Gutierrez, and R. Miranda, "CFD simulation gas-liquid flow in a copper converter with bottom air injection," *International Journal of Chemical Reactor Engineering*, vol. 6, article A54, 2008.

[12] D. Chibwe, G. Akdogan, Ch. Aldrich, and R. Eric, "CFD modelling of global mixing parameters in a Peirce-Smith converter with comparison to physical modelling," *Chemical Product and Process Modeling*, vol. 6, article 22, 2011.

[13] A. H.-L. Koohi, M. Halali, M. Askari, and M. T. Manzari, "Investigation and modeling of splashing in the Peirce Smith converter," *Chemical Product and Process Modeling*, vol. 3, no. 1, article 2, 2008.

[14] A. Valencia, R. Paredes, M. Rosales, E. Godoy, and J. Ortega, "Fluid dynamics of submerged gas injection into liquid in a model of copper converter," *International Communications in Heat and Mass Transfer*, vol. 31, no. 1, pp. 21–30, 2004.

[15] A. Valencia, M. Rosales, R. Paredes, C. Leon, and A. Moyano, "Numerical and experimental investigation of the fluid dynamics in a Teniente type copper converter," *International Communications in Heat and Mass Transfer*, vol. 33, no. 3, pp. 302–310, 2006.

[16] E. Delnoij, J. A. M. Kuipers, and W. P. M. Van Swaaij, "Computational fluid dynamics applied to gas-liquid contractors," *Chemical Engineering Science*, vol. 52, no. 21-22, pp. 3623–3638, 1997.

[17] Fluent 6.3 User's Guide, 2006.